ChemComm

COMMUNICATION

View Article Online
View Journal | View Issue

Published on 30 July 2014. Downloaded by UNIVERSITY OF OTAGO on 02/09/2014 03:38:55.

Cite this: *Chem. Commun.*, 2014, **50**, 10945

Received 7th July 2014,
Accepted 29th July 2014

DOI: 10.1039/c4cc05215c

www.rsc.org/chemcomm

Cyclometalated Ir(III) complexes as targeted theranostic anticancer therapeutics: combining HDAC inhibition with photodynamic therapy†

Rui-Rong Ye, Cai-Ping Tan,* Liang He, Mu-He Chen, Liang-Nian Ji and Zong-Wan Mao*

The successful design and anticancer mechanistic studies of a series of cyclometalated Ir(III) complexes with histone deacetylase inhibitory and photodynamic therapy (PDT) activities are reported.

Although cisplatin and its derivatives have gained great success, the development of platinum-based anticancer agents is hindered by many drawbacks, *e.g.*, serious side-effects and easily acquired drug resistance.[1] Recently, non-platinum-based compounds, such as iridium complexes, have attracted increasing attention in the search for alternatives to platinum-based metallo-anticancer drugs.[2] Multi-functional theranostic agents are expected to have significant clinical applications by integrating diagnosis and therapy simultaneously.[3] Due to their octahedral geometry, iridium complexes can be utilized to construct highly effective kinase inhibitors with high selectivity,[4] and the catalytic characteristics of iridium complexes endow them with interesting anticancer properties.[5] On the other hand, cyclometalated Ir(III) complexes are widely explored as bioimaging and biosensing agents due to their high quantum yields, large Stokes shifts, long-lived luminescence, good photostability and cell permeability.[6] These unique properties of cyclometalated Ir(III) complexes make them ideal candidates for constructing novel theranostic platforms.

Histone deacetylases (HDACs) regulate the expression and activity of many proteins in both cancer initiation and cancer progression by catalyzing the removal of acetyl groups from histones.[7] HDAC inhibitors (HDACis) show potent anticancer activities by promoting the acetylation of histones and non-histone proteins and inducing transcriptional events involved in growth arrest, differentiation, and apoptotic cell death.[8] Suberoylanilide hydroxamic acid (SAHA, vorinostat) is the first FDA-approved pan-HDACi that enters the clinic for treatment of cutaneous T-cell lymphoma. Several other organic molecule HDACis are now undergoing clinical trials.[9] Recently, some metal-based HDACis have been reported.[10]

Photodynamic therapy (PDT) is an attractive alternative for cancer treatment due to its high therapeutic efficacy and less side effects in comparison with radiotherapy and chemotherapy.[11] Upon irradiation, photosensitizers can cause the oxidative damage of tumor tissues by generating highly reactive singlet oxygen ($^1O_2$) and other reactive oxygen species (ROS).[12] PDT circumvents the lack of specificity of conventional therapies to some extent due to its inherent selectivity by localization of the photosensitizer to the tumor and confined toxicity due to spatial control of illuminated areas.[13] Metal complexes have become an attractive class of compounds for PDT with a diverse mechanism of action.[14] Recently, several groups reported that cyclometalated Ir(III) complexes can function as efficient sensitizers for PDT.[15]

In this study, we aim to achieve theranostic Ir(III)–HDACi hybrid complexes with synergistic inhibition effects on cancer cells due to their HDAC inhibitory potency and PDT activity. Four phosphorescent Ir(III) complexes, $[Ir(N\text{–}C)_2\mathbf{L}](PF_6)$ (**L** = N^1-hydroxy-N^8-(1,10-phenanthrolin-5-yl)octanediamide), which is a phenanthroline derivative modelled after SAHA; N–C = 2-phenylpyridine (ppy, **1**), 3-(2-pyridinyl)-coumarin (coumarin, **2**), 2-(2-thienyl)pyridine (thpy, **3**), and 2-(2,4-difluorophenyl)pyridine (dfppy, **4**) (Scheme 1), have been synthesized and characterized. Complexes **1–4** show potent inhibitory effects on HDACs. As a consequence, treatment of human cervical cancer (HeLa) cells with **1** leads to an elevation in histone-acetylation levels. Further mechanistic studies show that complex **1** can efficiently induce apoptosis in HeLa cells through HDAC inhibition and ROS elevation. Upon illumination with UV/visible light, the anti-cancer activities of **1–4** are greatly enhanced.

Ligand **L** was synthesized according to our previous work.[16] Complexes **1–4** were synthesized by reacting two equivalents of **L** with the Ir(III) chloro-bridged dimer. These complexes were characterized by ESI-MS, ^{1}H NMR and elemental analysis (Fig. S1–S4, ESI†).

The UV-vis absorption spectra of **1–4** in phosphate-buffered saline (PBS), CH_3CN and CH_2Cl_2 at 298 K are shown in Fig. S5 (ESI†).

MOE Key Laboratory of Bioinorganic and Synthetic Chemistry, School of Chemistry and Chemical Engineering, Sun Yat-sen University, Guangzhou 510275, P. R. China. E-mail: cesmzw@mail.sysu.edu.cn, tancaip@mail.sysu.edu.cn; Fax: +86-20-8411-2245

† Electronic supplementary information (ESI) available. See DOI: 10.1039/c4cc05215c

Published on 30 July 2014. Downloaded by UNIVERSITY OF OTAGO on 02/09/2014 03:38:55.

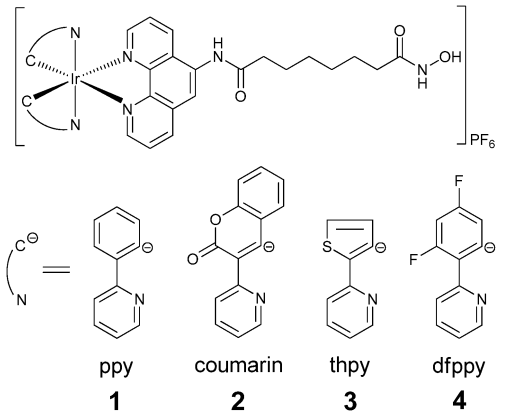

Scheme 1 The structures of complexes **1–4**.

The complexes display intense absorption bands at approximately 250–330 nm attributed to intraligand ($\pi \rightarrow \pi^*$) transitions and relatively weak bands at approximately 330–470 nm assigned to metal-to-ligand charge-transfer absorption.[17] The photophysical properties of complexes **1–4** are summarized in Table S1 (ESI†). Complexes **1–4** exhibit green to red emission in PBS, CH_3CN and CH_2Cl_2 under ambient conditions upon excitation at 405 nm (Fig. S6, ESI†).

$^1O_2$ is considered to be the main cytotoxic species in PDT. By using methylene blue (MB) as a standard, the quantum yields for $^1O_2$ production (Φ_Δ) of complexes **1–4** were evaluated in aerated dimethyl sulfoxide (DMSO) by monitoring the changes in the UV-vis spectra of 1,3-diphenylisobenzofuran (DPBF) at 418 nm.[15a,18] The rate of conversion of DPBF to 1,2-dibenzoylbenzene by $^1O_2$ is shown in Fig. S7 (ESI†) and the calculated Φ_Δ values are listed in Table S2 (ESI†). Under UV light irradiation, the Φ_Δ values increase in the order of **3** (0.21) < **2** (0.38) < **1** (0.45) < MB (0.52) < **4** (0.75). $^1O_2$ quantum yields were also determined for **1–4** upon illumination at 425 nm. It can be seen that $^1O_2$ can also be produced by **1–4** under visible light irradiation, which is more favourable for the application of PDT.

The rich photophysical properties of cyclometalated Ir(III) complexes can be utilized to study their cellular accumulation, trafficking and biodistribution, and they are ideal models to construct novel theranostic platforms integrating diagnostic and therapeutic purposes. It can be seen from confocal microscopy images that **1–4** can be effectively taken up by HeLa cells and are mainly retained within the cytoplasm after 5 h of incubation (Fig. S8, ESI†).

The cytotoxicity of **1–4** against several different cell lines (HeLa; human pulmonary carcinoma cell line A549; cisplatin-resistant cell line A549R; and human normal liver cell line LO2) was investigated both in the presence and absence of UV/visible light (Table 1; Tables S3 and S4, ESI†). The exposure of vehicle-treated cells to the light doses used does not induce the inhibition of cell proliferation. It can be seen that all Ir(III) complexes show moderate and selective cytotoxicity towards HeLa cells in the dark. However, a markedly increased cytotoxicity towards all cancer cells, including cisplatin-resistant A549 cells, is observed when cells are irradiated at 365 nm in the presence of **1–4** (IC_{50} = 3.1–21.9 μM). The phototoxicity index (PI) values of the compounds against HeLa cells follow the order: **1** (17.3) > **2** (16.2) > **3** (4.4) > **4** (2.7).

Table 1 (Photo)cytotoxicity of the compounds towards HeLa cells

	IC_{50} (μM)			PI[c]	
Compounds	Dark[a]	365 nm[b]	425 nm[b]	365 nm	425 nm
1	58.9 ± 3.3	3.4 ± 0.3	6.8 ± 0.9	17.3	8.7
2	50.1 ± 2.6	3.1 ± 0.3	4.5 ± 0.4	16.2	11.1
3	38.9 ± 3.0	8.9 ± 0.5	2.5 ± 0.2	4.4	15.6
4	30.2 ± 1.4	11.2 ± 1.0	1.6 ± 0.1	2.7	18.9
L	69.2 ± 5.4	65.3 ± 5.3	63.5 ± 4.3	1.1	1.1
SAHA	24.7 ± 2.3	23.6 ± 1.9	24.4 ± 1.1	1.0	1.0
Cisplatin	26.3 ± 1.5	22.4 ± 1.6	25.4 ± 1.6	1.2	1.0

[a] Cells were incubated with the indicated compounds in the dark for 48 h. [b] Cells were incubated with the indicated compounds for 12 h in the dark and then irradiated with light at 365 nm/425 nm. [c] PI = phototoxicity index; PI is the ratio of the IC_{50} values in the dark to those obtained upon light irradiation.

Complexes **1–4** also show phototoxicity when irradiated at 425 nm. The photo-induced cytotoxicity of these complexes is not well correlated with the quantum yields of $^1O_2$ production, which may imply that the overall result of photodynamic efficacy is influenced by many factors including cellular uptake levels, target binding affinity and $^1O_2$ production capability of photosensitizers in different intracellular environments. As expected, these complexes show much lower cytotoxicity against LO2 cells. Upon irradiation, the enhancement in the cytotoxicity of cisplatin, SAHA and ligand **L** is negligible, which indicates that the intracellular photo-induced toxicity mainly originates from the reaction between Ir(III) complexes and oxygen.

The HDAC inhibitory activities of complexes **1–4** were measured using a commercial HDAC activity assay kit by detecting the deacetylation of a synthetic fluorescent peptide.[19] As shown in Table 2 and Fig. S9 (ESI†), the inhibitory effects of compounds on HDAC activity are in the following order: **2** > SAHA > **3** > **L** > **1** > **4**. The result indicates that the conjugation of the HDAC-targeting ligand with cyclometalated Ir(III) moieties can retain or even improve the HDAC inhibitory activities.

Under 365 nm irradiation, **1** exhibits the strongest photodynamic response in HeLa cells, so it is chosen as the model compound to elucidate the anticancer mechanism, as well as the origin of the phototoxicity. Increased histone acetylation is an important marker of the cellular biological activity of the HDACis.[8] Western blot analysis of acetyl-histone H3 was performed to further determine whether HDACs were the cellular target of **1**. As shown in Fig. 1, the treatment of HeLa cells with **1** increases the acetylation level of histone H3 in a dose-dependent manner both in the absence and presence of light. Irradiated cells display higher histone H3

Table 2 *In vitro* inhibition of HeLa nuclear extract HDAC activity[a]

Compounds	IC_{50} (nM)
1	112.7 ± 8.5
2	39.0 ± 2.6
3	82.8 ± 6.1
4	665.2 ± 10.2
L	107.1 ± 8.2
SAHA	72.3 ± 5.5

[a] The results are mean ± standard deviation of three independent experiments.

 This journal is © The Royal Society of Chemistry 2014

Published on 30 July 2014. Downloaded by UNIVERSITY OF OTAGO on 02/09/2014 03:38:55.

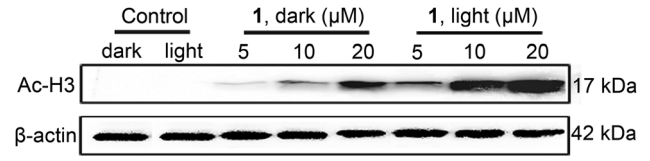

Fig. 1 Dose-dependent effect of complex **1** on the expression of acetyl-histone H3.

acetylation levels than cells in the dark, which indicates that light can enhance the HDAC inhibition capacity of **1** in cellular environments.

Apoptosis is reported to be the primary pathway for cell death execution of photodynamic cancer therapy as well as HDAC inhibition.[8,12,20] Induction of apoptosis by **1** was first studied by detecting changes in the cell morphology of HeLa cells. As shown in Fig. S10 (ESI†), treatment of cells with **1** results in an increase (control: 2.5 ± 0.3%; 10 μM **1**: 14.2 ± 1.6%; 20 μM **1**: 26.7 ± 1.2%) in the percentage of cells with abnormal nuclear morphology, *e.g.*, chromatin condensation and nuclear fragmentation. In the presence of 365 nm light, a significant increase in the proportion of cells with abnormal nucleus is observed (control: 3.2 ± 0.2%; 10 μM **1**: 30.4 ± 2.1%; 20 μM **1**: 70.6 ± 4.3%). Similar results are obtained by annexin-V labelling, detecting phosphatidylserine externalization, a hallmark of the early phase of apoptosis.[21] Flow cytometric analysis shows that treatment of HeLa cells with **1** in the absence of light leads to a concentration-dependent increase in the percentage of cells that are annexin-V positive (control: 3.6 ± 0.8%; 10 μM **1**: 10.0 ± 0.9%; 20 μM **1**: 24.3 ± 2.0%) (Fig. 2). Upon illumination, a marked increase in the percentage of HeLa cells that are annexin-V positive is observed (control: 4.5 ± 0.3%; 10 μM **1**: 25.1 ± 1.3%; 20 μM **1**: 75.4 ± 4.8%). The fluorescence microscopy experiment also shows that light irradiation can greatly increase the percentage of apoptotic cells induced by treatment with **1** (Fig. S11, ESI†).

Caspases have been identified as key executors of apoptosis under various stimuli, and the activation of capase-3 is considered to be a marker of apoptosis.[22] As shown in Fig. S12A (ESI†), treatment of HeLa cells with **1** results in a concentration-dependent increase in caspase-3/7 activity in the dark. At the same time, light can greatly increase the activation of caspase-3/7 caused by treatment with **1**. Accordingly, the well-known

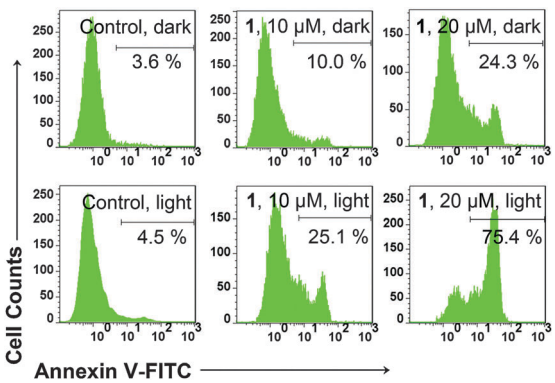

Fig. 2 Characterization of apoptosis induced by complex **1** using annexin V-FITC staining.

substrate of activated caspase-3 involved in apoptotic signaling, poly(ADP-ribose) polymerase (PARP),[23] is cleaved to an 85 kD signature peptide (PARP-CF) in **1**-treated HeLa cells in a dose-dependent manner, and light can further elevate the percentage of cleaved PARP (Fig. S12B, ESI†).

To further elucidate the mechanisms of **1**-induced growth inhibition, the effect of **1** on cell cycle distribution was studied by flow cytometry in HeLa cells. No obvious disturbance in cell cycle distribution is observed both in the dark and under light irradiation (Table S5, ESI†). In the presence of **1**, irradiated cells show a marked increase in the proportion of apoptotic cells compared with those in the dark, as indicated by the increase in sub-G1 peaks.[24]

ROS, particularly $^1O_2$, are the most important mediators of cell death induced by PDT.[12] The effect of **1** on intracellular ROS levels was examined by 2′,7′-dichlorofluorescein (DCF) fluorescence assay using confocal microscopy and flow cytometry. A moderate concentration-dependent increase of ROS is observed in HeLa cells treated with **1** for 6 h in the dark, and illumination at 365 nm can greatly improve the capability of **1** to produce ROS (Fig. S13A and B, ESI†). Under irradiation, treatment of **1** at 40 μM resulted in ~5-fold higher fluorescence signals compared with the vehicle-treated cells.

ROS elevation and mitochondrial dysfunction are two closely related events. During apoptosis, several key events occur in mitochondria, including the release of caspase activators and the loss of mitochondrial membrane potential (MMP, $\Delta\Psi_m$).[25] Therefore, confocal microscopy and flow cytometry were used to confirm whether **1**-induced apoptosis occurred through damaging mitochondria using 5,5′,6,6′-tetrachloro-1,1′,3,3′-tetraethylbenzimidazolylcarbocyanine iodide (JC-1) as the MMP-sensitive probe. As shown in Fig. S14A (ESI†), in the presence of **1**, light-irradiated cells display a more significant red to green color shift indicating the loss of MMP compared with cells treated in the dark. Representative JC-1 red/green ratio signals recorded by flow cytometry are shown in Fig. S14B (ESI†). Under dark conditions, a concentration-dependent decrease in the red/green fluorescence intensity ratios can be detected (control: 54.6 ± 2.2; 20 μM **1**: 43.6 ± 3.1; 40 μM **1**: 32.4 ± 2.2). PDT treatment markedly decreases the ratios of red to green fluorescence (control: 54.7 ± 1.4; 20 μM **1**: 18.1 ± 1.5; 40 μM **1**: 5.4 ± 0.4).

In summary, a series of cyclometalated Ir(III) complexes as HDACis and photodynamic therapeutic agents have been explored. Upon UV (365 nm) or visible (425 nm) light irradiation, complexes **1–4** show potent cytotoxicity towards the cancer cell lines screened, and display much lower phototoxicity against human normal cells. Mechanistic studies show that **1** induces apoptotic cell death mainly through inhibition of HDACs, ROS production and mitochondrial damage. Under UV light irradiation, the biological effects of **1** mentioned above are significantly enhanced. Our study demonstrates that the combination of the molecular targeted drug design methodology with the PDT potential of phosphorescent Ir(III) complexes may be a very useful strategy to develop novel tumor-oriented multifunctional metallo-anticancer therapeutics.

This work is supported by National Natural Science Foundation of China (No. 21172274, 21231007, 21121061, 21201183

Published on 30 July 2014. Downloaded by UNIVERSITY OF OTAGO on 02/09/2014 03:38:55.

and J1103305), State High-Tech Development Program (863 Program: 2012AA020305), the Ministry of Education of China (No. 20100171110013 and 313058), the National Basic Research Program of China (973 Program No. 2014CB845604) and the Fundamental Research Funds for the Central Universities.

Notes and references

1 L. Galluzzi, L. Senovilla, I. Vitale, J. Michels, I. Martins, O. Kepp, M. Castedo and G. Kroemer, *Oncogene*, 2012, **31**, 1869.
2 C. H. Leung, H. J. Zhong, D. S. H. Chan and D. L. Ma, *Coord. Chem. Rev.*, 2013, **257**, 1764.
3 (*a*) D. Can, B. Spingler, P. Schmutz, F. Mendes, P. Raposinho, C. Fernandes, F. Carta, A. Innocenti, I. Santos, C. T. Supuran and R. Alberto, *Angew. Chem., Int. Ed.*, 2012, **51**, 3354; (*b*) S. Maiti, N. Park, J. H. Han, H. M. Jeon, J. H. Lee, S. Bhuniya, C. Kang and J. S. Kim, *J. Am. Chem. Soc.*, 2013, **135**, 4567.
4 (*a*) A. Wilbuer, D. H. Vlecken, D. J. Schmitz, K. Kräling, K. Harms, C. P. Bagowski and E. Meggers, *Angew. Chem., Int. Ed.*, 2010, **49**, 3839; (*b*) L. Feng, Y. Geisselbrecht, S. Blanck, A. Wilbuer, G. E. Atilla-Gokcumen, P. Filippakopoulos, K. Kräling, M. A. Celik, K. Harms, J. Maksimoska, R. Marmorstein, G. Frenking, S. Knapp, L.-O. Essen and E. Meggers, *J. Am. Chem. Soc.*, 2011, **133**, 5976.
5 Z. Liu, I. Romero-Canelon, B. Qamar, J. M. Hearn, A. Habtemariam, N. P. E. Barry, A. M. Pizarro, G. J. Clarkson and P. J. Sadler, *Angew. Chem., Int. Ed.*, 2014, **53**, 3941.
6 (*a*) K. K.-W. Lo, B. T.-N. Chan, H.-W. Liu, K. Y. Zhang, S. P.-Y. Li and T. S.-M. Tang, *Chem. Commun.*, 2013, **49**, 4271; (*b*) Y. You, Y. Han, Y. M. Lee, S. Y. Park, W. Nam and S. J. Lippard, *J. Am. Chem. Soc.*, 2011, **133**, 11488.
7 S. Minucci and P. G. Pelicci, *Nat. Rev. Cancer*, 2006, **6**, 38.
8 E. Seto and M. Yoshida, *Cold Spring Harbor Perspect. Biol.*, 2014, **6**, a018713.
9 P. A. Marks and R. Breslow, *Nat. Biotechnol.*, 2007, **25**, 84.
10 (*a*) J. Spencer, J. Amin, M. Wang, G. Packham, S. S. S. Alwi, G. J. Tizzard, S. J. Coles, R. M. Paranal, J. E. Bradner and T. D. Heightman, *ACS Med. Chem. Lett.*, 2011, **2**, 358; (*b*) J. Spencer, J. Amin, R. Boddiboyena, G. Packham, B. E. Cavell, S. S. Syed Alwi, R. M. Paranal, T. D. Heightman, M. Wang, B. Marsden, P. Coxhead, M. Guille, G. J. Tizzard, S. J. Coles and J. E. Bradner, *MedChemComm*, 2012, **3**, 61; (*c*) J. d. J. Cazares Marinero, M. Lapierre, V. Cavailles, R. Saint-Fort, A. Vessieres, S. Top and G. Jaouen, *Dalton Trans.*, 2013, **42**, 15489.
11 D. Dolmans, D. Fukumura and R. K. Jain, *Nat. Rev. Cancer*, 2003, **3**, 380.
12 P. Agostinis, K. Berg, K. A. Cengel, T. H. Foster, A. W. Girotti, S. O. Gollnick, S. M. Hahn, M. R. Hamblin, A. Juzeniene, D. Kessel, M. Korbelik, J. Moan, P. Mroz, D. Nowis, J. Piette, B. C. Wilson and J. Golab, *Ca-Cancer J. Clin.*, 2011, **61**, 250.
13 J. P. Celli, B. Q. Spring, I. Rizvi, C. L. Evans, K. S. Samkoe, S. Verma, B. W. Pogue and T. Hasan, *Chem. Rev.*, 2010, **110**, 2795.
14 (*a*) Y. Zhao, N. J. Farrer, H. Li, J. S. Butler, R. J. McQuitty, A. Habtemariam, F. Wang and P. J. Sadler, *Angew. Chem., Int. Ed.*, 2013, **52**, 13633; (*b*) A. Naik, R. Rubbiani, G. Gasser and B. Spingler, *Angew. Chem., Int. Ed.*, 2014, **53**, 6938; (*c*) R. Lincoln, L. Kohler, S. Monro, H. Yin, M. Stephenson, R. Zong, A. Chouai, C. Dorsey, R. Hennigar, R. P. Thummel and S. A. McFarland, *J. Am. Chem. Soc.*, 2013, **135**, 17161; (*d*) A. Kastl, S. Dieckmann, K. Wähler, T. Völker, L. Kastl, A. L. Merkel, A. Vultur, B. Shannan, K. Harms, M. Ocker, W. J. Parak, M. Herlyn and E. Meggers, *ChemMedChem*, 2013, **8**, 924; (*e*) A. Leonidova, V. Pierroz, R. Rubbiani, J. Heier, S. Ferrari and G. Gasser, *Dalton Trans.*, 2014, **43**, 4287; (*f*) A. Leonidova, V. Pierroz, R. Rubbiani, Y. Lan, A. G. Schmitz, A. Kaech, R. K. O. Sigel, S. Ferrari and G. Gasser, *Chem. Sci.*, 2014, DOI: 10.1039/C3SC53550A; (*g*) B. S. Howerton, D. K. Heidary and E. C. Glazer, *J. Am. Chem. Soc.*, 2012, **134**, 8324; (*h*) M. A. Sgambellone, A. David, R. N. Garner, K. R. Dunbar and C. Turro, *J. Am. Chem. Soc.*, 2013, **135**, 11274.
15 (*a*) S. P.-Y. Li, C. T.-S. Lau, M.-W. Louie, Y.-W. Lam, S. H. Cheng and K. K.-W. Lo, *Biomaterials*, 2013, **34**, 7519; (*b*) Y. You and W. Nam, *Chem. Soc. Rev.*, 2012, **41**, 7061; (*c*) A. Kastl, A. Wilbuer, A. L. Merkel, L. Feng, P. Di Fazio, M. Ocker and E. Meggers, *Chem. Commun.*, 2012, **48**, 1863.
16 R.-R. Ye, Z.-F. Ke, C.-P. Tan, L. He, L.-N. Ji and Z.-W. Mao, *Chem. – Eur. J.*, 2013, **19**, 10160.
17 S. Serroni, A. Juris, S. Campagna, M. Venturi, G. Denti and V. Balzani, *J. Am. Chem. Soc.*, 1994, **116**, 9086.
18 N. Adarsh, R. R. Avirah and D. Ramaiah, *Org. Lett.*, 2010, **12**, 5720.
19 C. Haumaitre, O. Lenoir and R. Scharfmann, *Mol. Cell. Biol.*, 2008, **28**, 6373.
20 N. L. Oleinick, R. L. Morris and T. Belichenko, *Photochem. Photobiol. Sci.*, 2002, **1**, 1.
21 Z. Bacsó, R. B. Everson and J. F. Eliason, *Cancer Res.*, 2000, **60**, 4623.
22 J. Li and J. Yuan, *Oncogene*, 2008, **27**, 6194.
23 F. J. Oliver, G. de la Rubia, V. Rolli, M. C. Ruiz-Ruiz, G. de Murcia and J. M.-d. Murcia, *J. Biol. Chem.*, 1998, **273**, 33533.
24 P. Karna, S. Sharp, C. Yates, S. Prakash and R. Aneja, *Mol. Cancer*, 2009, **8**, 93.
25 C. Wang and R. J. Youle, *Annu. Rev. Genet.*, 2009, **43**, 95.

 This journal is © The Royal Society of Chemistry 2014